Pressure Dependence of the Structures of Carbonaceous Deposits Formed by Laser Ablation on Targets Composed of Carbon, Nickel, and Cobalt

M. Yudasaka,*,† T. Komatsu,† T. Ichihashi,† Y. Achiba,‡ and S. Iijima†

NEC Corporation, 34 Miyukigaoka, Tsukuba, Ibaraki 305, Japan, and Department of Chemistry, Tokyo Metropolitan University, Minami-oosawa Hachioji, Tokyo 192-03, Japan

Received: October 24, 1997; In Final Form: April 20, 1998

The structures of carbonaceous deposits obtained through laser ablations using targets composed of C, Ni, and Co under various Ar gas pressures were studied. The pressure dependence of the target's surface morphology and the structure was also studied. When the pressure was 100 Torr or below, only carbon was evaporated from the target and amorphous carbon was formed during the laser ablation. When the pressure was 200 Torr or higher, both carbon and metal was evaporated and single-wall carbon nanotubes and amorphous carbon were formed during the laser ablation. A mechanism of the single-wall carbon nanotube formation by laser ablation is proposed.

Introduction

Two types of carbon nanotubes, the multiwall carbon nanotube (MCNT)[1] and the single-wall carbon nanotube (SCNT)[2] are known. An MCNT can be made by chemical vapor deposition (CVD)[3] and arc discharge.[4,5] The formation mechanism of MCNTs by CVD has been well-investigated;[3,6] a particle of the metal catalyst takes a particular size and grows an MCNT where the particle of the metal catalyst exists either at the top or the bottom of the MCNT.[7−9]

SCNTs have been reported to have been made by arc discharge,[2] laser ablation,[10] and CVD.[8] A high yield of SCNTs, above 70%, has been attained by arc discharge[11] and laser ablation.[10] In these three methods, a metal catalyst is essential to form an SCNT, but the role of the metal in SCNT formation has not been clarified yet. It has been suggested that one metal atom can form an SCNT in the laser ablation.[10] In situ observation of SCNT formation is not easy, though, because of the high temperatures of around 1200 °C needed to form SCNTs by laser ablation. In the work reported here, we studied the strucutres of the carbonaceous deposits and target surfaces to elucidate the mechanism of the SCNT formation by laser ablation.

Experimental Section

The chamber used for the laser ablation was a quartz glass tube with an inside diameter of about 3.6 cm and a length of 60 cm. Another quartz tube with an inside diameter of about 2.7 cm and a length of 50 cm was located at the center of the chamber. A target was placed inside, at the center of the inner quartz glass tube. A quartz glass plate was situated in front of the target. The temperature at the center of the target was controlled to be 1200 °C. The temperature at the outlet edge of the inner quartz glass tube was about 500 °C. Argon gas flowed through the tubes at a rate of 0.5 L/min. The pressure inside the chamber was controlled to values between 4 and 600 Torr by using a rotary pump.

A pulsed laser beam from a Nd:YAG laser (wavelength = 532 nm, pulse width = 6−7 ns, repetition = 10 Hz) irradiated the target surface perpendicularly through a quartz glass window of the chamber. The laser beam intensity was 2 W, and the beam diameter was 5 mm. The period of the laser beam irradiation was 1 min. The direction of the laser beam irradiation was the same as that of the Ar gas flow. A part of the products formed by the laser ablation was deposited on the quartz glass plates located in front of the target, and the remaining products flowed down to the rear of the target.

Results and Discussion

The Raman spectrum of the target surface before the laser ablation (Figure 1a) has a sharp peak at 1583 cm^{-1} and a small peak at 1369 cm^{-1}. The former peak is characteristic of graphite, and the latter appears when the basal domain size of the graphite is small.[12] The Raman spectrum of Figure 1a indicates that the carbon used in the target has a graphite structure with a small basal domain size. After the target was laser-ablated, the Raman spectrum of the target changed and exhibited two broad peaks at around 1600 and 1360 cm^{-1} (Figure 1b−g). The intensity of the broad peak at around 1360 cm^{-1} relative to that of the broard peak at around 1600 cm^{-1} becomes greater as the pressure increases (Figure 1b−d). These two broad peaks are similar to those of amorphous carbon (a-C).[12] This indicates that the target surface was decomposed by the laser beam and transformed into a-C, and the degree of decomposition tended to increase as the pressure became higher.

The Ar gas pressure dependence of the Raman spectra of the carbonaceous deposits formed by the laser ablation on the quartz glass plates located in front of the target is shown in Figure 2. When the pressure is 4 or 100 Torr, the spectrum of the carbonaceous deposit shows two broad peaks of a-C. When the pressure was 200 Torr or above, the Raman spectrum of the carbonaceous deposit on the quartz glass plate shows a sharp peak at around 1590 cm^{-1} and shoulders or peaks at around 1570 cm^{-1}. These peaks indicate the existence of SCNT because the peak positions and relative intensities are close to those of SCNT.[13] The other peak characteristic of SCNT that should appear between 160 and 200 cm^{-1} can be seen at 170

* Corresponding author. E-mail: yudasaka@sci.cl.nec.co.jp.
† NEC Corporation.
‡ Tokyo Metropolitan University.

S1089-5647(97)03446-9 CCC: $15.00
Published on Web 06/05/1998

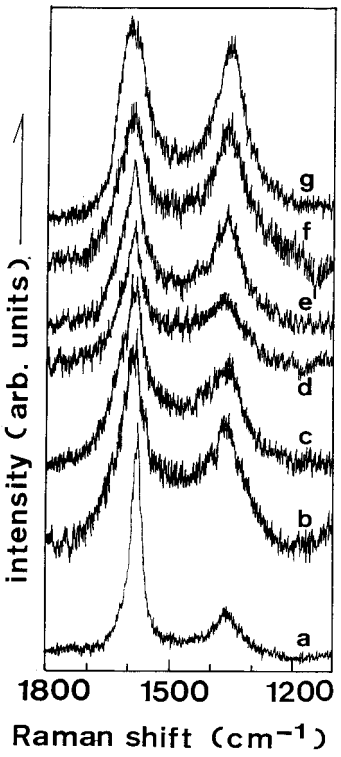

Figure 1. Raman spectra of targets before (a) and after laser ablation under pressures of 4 (b), 100 (c), 200 (d), 300 (e), 400 (f), and 500 Torr (g).

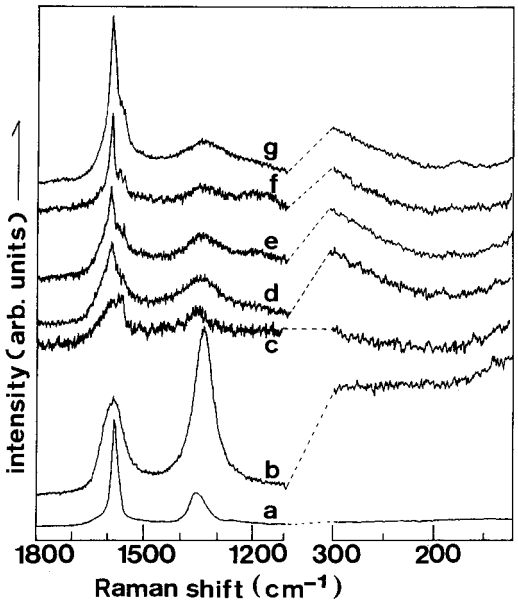

Figure 2. Raman spectra (excitation wavelength = 524.5 nm) of target before the laser ablation (a) and carbonaceous deposits formed by laser ablation on quartz glass plates located in front of target at pressures of 4 (b), 100 (c), 200 (d), 300 (e), 400 (f), and 500 Torr (g).

cm^{-1} in Figure 2 but not in Figure 2d−f. This absence of the peak is due to its weak intensity[13] and the small quantity of SCNT contained in the film. The intensities of the peaks at 1590 cm^{-1} and shoulders or peaks at around 1570 cm^{-1} increase relative to the intensities of the two broad a-C peaks as the pressure increases (Figure 2d−f). This indicates that the SCNT can be formed at pressures above 200 Torr, and its quantity relative to that of a-C becomes larger as the pressure increases. The origin of the shoulders at around 1570 cm^{-1} in Figure 2c is not apparent.

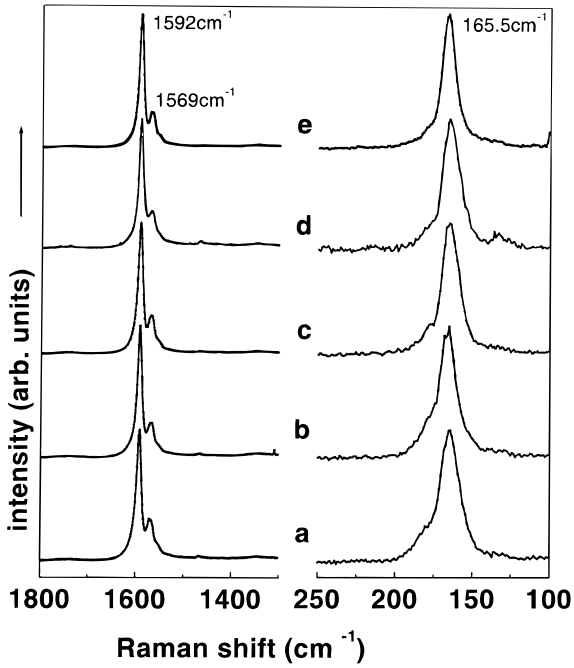

Figure 3. Raman spectra (excitation wavelength = 488 nm) of spider-web-like deposits obtained at exit of liner tube by laser ablation at pressures of 200 (a), 300 (b), 400 (c), 500 (d), and 600 Torr (e).

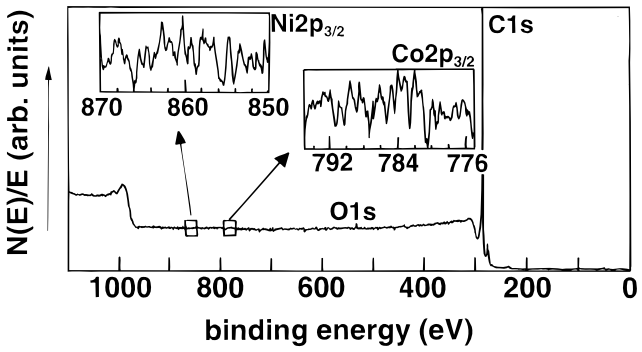

Figure 4. XPS spectra of carbonaceous deposit formed on quartz glass plate at a pressure of 4 Torr.

Almost no carbonaceous deposits were found at the exit of the inner tube when the Ar gas pressures were 4 and 100 Torr. However, a spider-web-like carbonaceous deposit appeared at the exit of the inner quartz tube when the pressure was 200 Torr or above. A quantity of spider-web-like carbonaceous deposits increased as the pressure increased. The Raman spectra of the spider-web-like deposits are shown in Figure 3. Each spectrum has three sharp peaks at around 1592, 1569, and 165.5 cm^{-1}. These three peaks are characteristic of SCNTs;[13] therefore, the spider-web-like deposit clearly includes SCNT material.

X-ray photoelectron spectroscopy (XPS) revealed the components of the carbonaceous deposits formed on the quartz glass plate at 4 or 100 Torr. Here, a target containing 9% metal (Ni + Co) was used to form the carbonaceous deposits on the quartz glass plate in front of the target. No peak corresponding to Ni or Co appeared in the XPS spectrum from the deposit formed at 4 Torr. (Figure 4) or the deposit formed at 100 Torr. This indicates that the concentration of Ni or Co in the carbonaceous deposits on the quartz glass plate was less than 1%. Clearly very little of Ni or Co was evaporated from the target by the laser ablation at a pressure of 4 or 100 Torr. This is the major reason why a-C was formed and almost no SCNT was found on the quartz glass plate at these pressures.

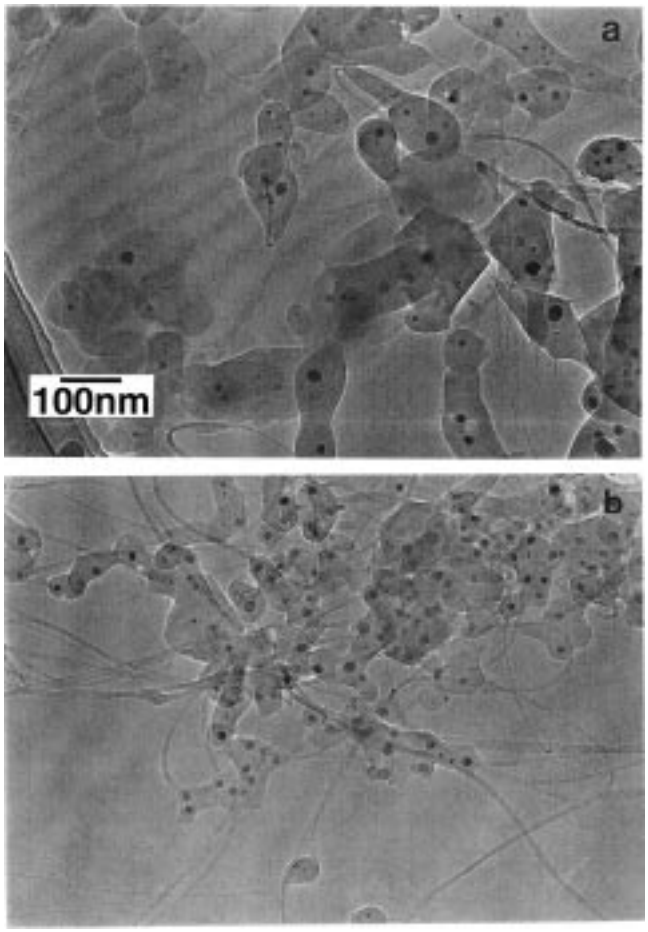

Figure 5. TEM images of spider-web-like deposit obtained by laser ablation at pressures of 200 (a) and 600 Torr (b).

We also studied the structure of the spider-web-like deposit by transmission electron microscopy (TEM). TEM images of the spider-web-like deposits formed at 200 Torr are shown in Figure 5a. Figure 5a shows three kinds of feature: fibers, generally rounded large particles, and small round particles located within the large rounded particles. Many of the fibers grow from the rounded particles. The fibers were 1−100 nm thick. Magnified TEM images of the thick fibers showed that they consisted of bundles of thin fibers about 1 nm thick that were covered by a-C. We consider these fibers to be SCNTs judging from the Raman spectra in Figure 3 and refs 10 and 13. The large rounded particles are about 100 nm across their widest point. The small round particles are 1−50 nm across. Energy dispersion X-ray spectroscopy indicated that the fibers and the large rounded particles are made of carbon and the small round particles inside the large ones are made of mixture of Ni and Co. No graphite lattice structure could be seen in Figure 5a.

A TEM image of the spider-web-like carbonaceous deposit obtained at the Ar gas pressure of 600 Torr is shown in Figure 5b. In Figure 5b, the a-C takes on an amoeba-like shape and the SCNTs form thick bundles. The quantity of a-C in Figure 5b is apparently less than that in Figure 5a. The high pressure results in a large quantity of SCNTs consisting of the thick bundles of SCNTs and less a-C.

These results indicate that SCNTs are formed at 200 Torr and above, where not only C but also a considerable quantity of Ni and Co are evaporated from the target by the laser ablatiion. In this report, the threshold pressure for the formation of the spider-web-like deposit containing SCNTs is 200 Torr. (However, in previous experiments, we have found that this threshold pressure approaches 100 Torr when longer laser ablation time and/or a higher metal concentration in the target are used.)

The fact that the metal evaporation from the target requires a high Ar gas pressure was reflected in the SEM images of the laser-ablated surfaces of the target (Figure 6). The SEM image of the target surface before the laser ablation showed dark regions of graphite powders and white regions of metal particles (Figure 6a). The SEM image of the surface that was laser-ablated at a pressure of 4 Torr exhibits carbon-mountains capped by metal (Figure 6b). As the pressure increased, the metal cap decreased in area (Figure 6c), and almost no metal caps could be seen when the pressure was 600 Torr (Figure 6d). These SEM images show that Ni and Co were evaporated more readily at higher pressures.

One possible explanation of why the Ni and Co evaporated more easily at higher pressures is as follows. Carbon would absorb the pulsed laser beam, transforming the laser beam energy into thermal energy. As a result, the carbon would become "hot" carbon whose temperature is known to rise above 4000 °C where it takes the liquid state.[14,15] On the other hand, a metal would reflect the laser beam, limiting its temperature increase. When the pressure was 4 or 100 Torr, the hot carbon would have evaporated quickly without transferring its thermal energy to the Ni or Co. Therefore, most of the Ni and Co did not evaporate and remained on the target surface. When the pressure was 200 Torr or above, the evaporation rate of the hot carbon would fall because the evaporated carbon would more frequently return to the target surface. Therefore, the amount of the hot carbon that could interact with Ni and Co would have increased, and the thermal energy of the carbon would be transferred to the Ni and Co. As a result of this energy transfer, carbon, nickel, and cobalt would form a liquid-like mixture at the target surface, and not only carbon but also nickel and cobalt would be removed from the target surface by the laser ablation at higher pressures.

The Ar gas pressure dependence of SCNT formation by the laser ablation described above indicates that a difference in pressure results in a difference in the metal concentration of the material removed from the target surface. To find the correlation between the SCNT formation and the metal concentration explicitly, we used two targets with different metal concentrations. Figure 5b shows the TEM image of the spider-web-like deposits formed when using targets with the metal (Ni and Co) concentration of 1.2%. Figure 7 shows the TEM images of the spider-web-like deposits formed when using targets with the metal (Ni and Co) concentrations of 9%. In Figures 5b and 7, the quantity of SCNT material relative to that of a-C becomes smaller and the bundles become thicker when the metal concentration is 9%. Therefore, the metal concentration clearly affects the yield and bundle thickness of the SCNTs.

A model for the SCNT formation mechanism must explain the several characteristics of SCNTs: the SCNT diameter of around 1 nm,[10] the appearance of SCNTs as bundles in which the SCNTs take the closed packing configuration,[10] the branches of the bundle,[10] and the dependence of the bundle thickness on the metal quantity.

A possible mechanism that accounts for the SCNT formation by laser ablation can be deduced from the experimental findings described in this report as follows. The C, Ni, and Co at the target surface would be made into a molten mixture by the laser ablation at a pressure of 200 Torr or higher as described above.

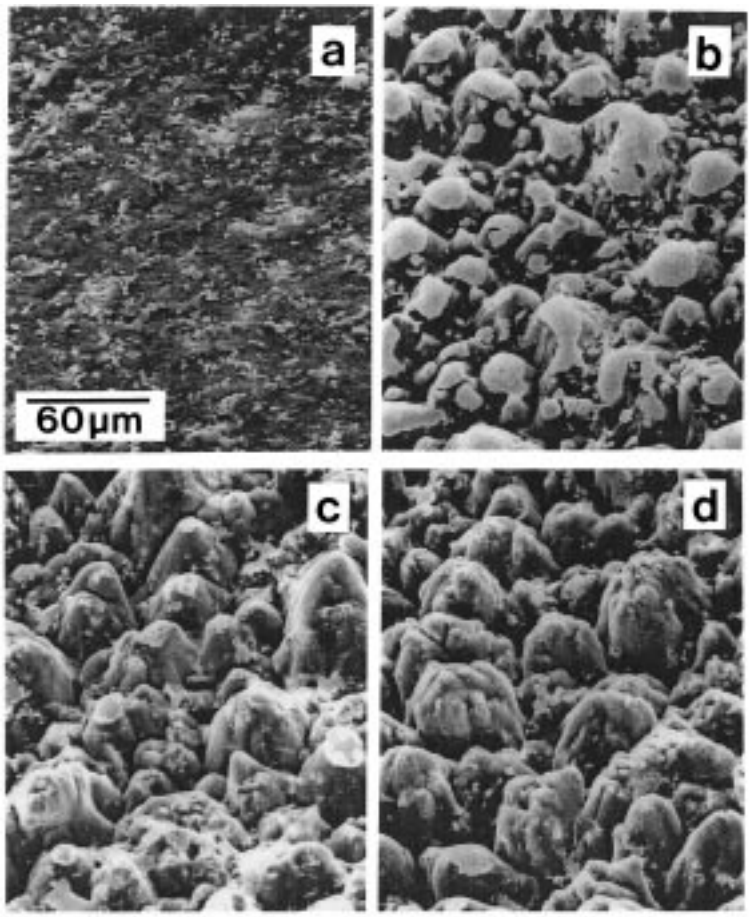

Figure 6. SEM images of target before the laser ablation (a) and after laser ablation at pressures of 4 (b), 400 (c), and 600 Torr (d).

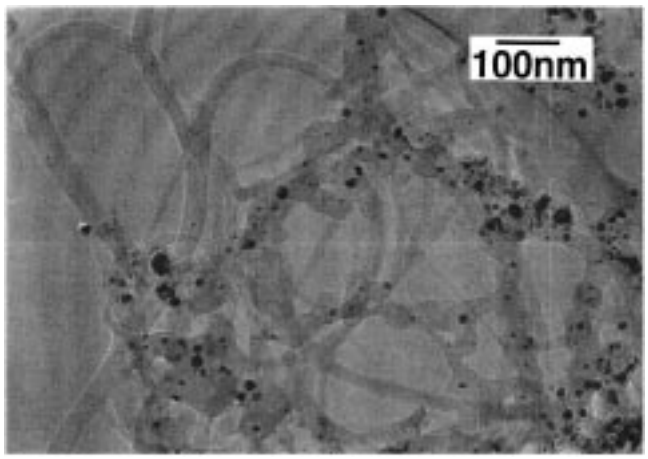

Figure 7. TEM image of spider-web-like deposit formed by laser ablation using target with metal (Ni + Co) concentration of 9%.

C, Ni, and Co would then be removed from the molten target surface as vapor or as molten particles, as described in ref 16, which provides a general review on pulsed laser deposition. The molten particles, in which C, Ni, and Co would mix homogeneously, would remain at the high temperature immediately after they were removed from the target surface, but their temperature would fall as the molten particle moved away from the target surface. This temperature decrease would cause the segregation of Ni and Co in the particle, leading to the formation of metal (Ni and Co) clusters surrounded by carbon. When the metal cluster size becomes large enough to catalyze the SCNT formation, it would form an SCNT using the carbon surrounding it.

Reference 8 reports that Co particles, whose diameter is controlled by zeolite pores with diameters of around 1 nm, can form SCNTs. Reference 17 showed that wide tubes initially open can continue to grow straight; however, tubes narrower than about 3 nm lead to closure. This closure is prevented by small metal particle, which is shown by calculation using a 1.0-nm-diameter SCNT. From these reports, it is likely that metal clusters with diameters around 1 nm form SCNTs with diameters influenced by the metal cluster size.

When the metal concentration inside the molten particle is high, the metal cluster concentration, and therefore, the SCNT concentration, increases. This may explain the thicker SCNT bundle formation when the metal concentration of the target surface or of the target itself is high. The formation of the branches of the SCNT bundles might be related to the increase in the metal cluster concentration (owing to the temperature decrease and carbon consumption for the SCNT formation) and to collisions among the particles and the bundles.

The model for SCNT formation described above needs further confirmation. For example, the dependence that the metal cluster catalyst's ability to form SCNTs and MCNTs on the metal cluster size needs to be clearly shown. The model will become more believable if the intermediate state of an SCNT growing from a metal cluster with a size around 1 nm can be observed explicitly.

Another possible mechanism of SCNT formation by laser ablation is similar to that of fullerene formation. The pressure dependence of the yield of fullerenes formed by laser ablation using a target of metal-free carbon studied in detail.[18] The fullerene yield increased above 100 Torr when the laser ablation temperature was kept at around 1000 °C.[18] This trend is similar

to the pressure dependence of the SCNT yield described in this report. The fullerene precursers may be the same as the precursers that enable SCNT formation by the laser ablation.

Acknowledgment. The research was undertaken under the NEDO International Joint Research Program, Special Funds of the Science and Technology Agency of the Japanese Government, and Research Project for the Future of the Japan Society for the Promotion of Science in Ministry of Education of Japanese Government.

References and Notes

(1) Iijima, S. *Nature* **1991**, *354*, 56.
(2) Iijima, S.; Ichihashi, T. *Nature* **1993**, *363*, 603.
(3) Endo, M.; Takeuchi, K.; Kobori, K.; Takahashi, K.; Kroto, H. W.; Sarkar, A. *Carbon* **1995**, *33*, 873.
(4) Bacon, R. *J. Appl. Phys.* **1990**, *34*, 283.
(5) Ebbesen, T. W.; Ajayan, P. M. **1992**, *358*, 220.
(6) Tibbetts, G. G. *J. Cryst. Growth* **1984**, *66*, 632.
(7) Yudasaka, M.; Kikuchi, R.; Matsui, T.; Ohki, Y.; Ota, E.; Yoshimura, S. *J. Appl. Phys.* **1995**, *67*, 2477.
(8) Fonseca, A.; Hernadi, K.; Piedigrosso, P.; Biro, L. P.; Lazarescu, S. D.; Lambin, Ph.; Thiry, P. A.; Bernaerts, D.; Nagy, J. B. *Proceedings of Fullerenes: Chemistry, Physics, and New Directions IX*; The Electrochemistry Society Inc.: Montreal, 1997.
(9) Yudasaka, M.; Kikuchi, R.; Ohki, Y.; Yoshimura, S. *Carbon* **1997**, *35*, 195.
(10) Guo, T.; Nikolaev, P.; Thess, A.; Colbert, D. T.; Smalley, R. E. *Chem. Phys. Lett.* **1995**, *243*, 49. Thess, A.; Lee, R.; Nikolaev, P.; Dai, H.; Petit, P.; Robert, J.; Xu, C.; Lee, Y. H.; Kim, S. G.; Rinzler, A. G.; Tomanek, D.; Fisher, L. E.; Smalley, R. E. *Science* **1996**, *273*, 483.
(11) Journet, C.; Maser, W. K.; Bernier, P.; Loiseau, A.; Lamy, M.; de la Chapelle, M. Lamy; Lefrant, S.; Deniard, P.; Lee, R.; Fisher, J. E. *Nature* **1997**, *388*, 756.
(12) Kinoshita, K. *Carbon, Electrochemical and Physicochemical Properties, 3*; John Wiley & Sons: New York, 1988; Chapter 2.2.
(13) Rao, A. M.; Richter, E.; Bandow, Shunji; Chase, B.; Eklund, P. C.; Wiliams, K. A.; Fang, S.; Subbaswamy, K. R.; Menon, M.; Thess, A.; Smalley, R. E.; Dresselhaus, G.; Dresselhaus, M. S. *Science* **1997**, *275*, 187.
(14) Steinback, J.; Braunstein, G.; Dresselhaus, M. S.; Venkatesan, T.; Jacobson, D. C. *J. Appl. Phys.* **1988**, *58*, 4374.
(15) Achiba, Y. Private communication.
(16) Cheung, J.; Horwitz, J. *MRS Bull.* **1992**, *18*, 30.
(17) Maiti, A.; Brabec, C. J.; Roland, C.; Bernhole, J. *Phys. Rev.* **1995**, *52*, 14850.
(18) Wakabayashi, T.; Kasuya, D.; Shiromaru, H.; Suzuki, S.; Kikuchi, K.; Achiba, Y. *Z. Phys. D* **1997**, *40*, 414.